

Lawrence Berkeley National Laboratory

LBL Publications

Title

Synthase-Selective Exploration of a Tunicate Microbiome by Activity-Guided Single-Cell Genomics

Permalink

<https://escholarship.org/uc/item/3pj1p4hn>

Journal

ACS Chemical Biology, 16(5)

ISSN

1554-8929

Authors

Kim, Woojoo E
Charov, Katherine
Džunková, Mária
et al.

Publication Date

2021-05-21

DOI

10.1021/acscchembio.1c00157

Peer reviewed

1
2
3 **Letter**
4
5
6
7
8

9 **Synthase–selective exploration of a tunicate microbiome by activity–**
10 **guided single–cell genomics**
11
12
13
14
15
16

17 Woojoo E. Kim,^{1,†} Katherine Charov,^{1,†} Mária Džunková,^{2,†} Eric D. Becraft,^{3,4,†} Julia Brown,^{3,†}
18 Frederik Schulz,² Tanja Woyke,² James J. La Clair,¹ Ramunas Stepanauskas^{3,*} & Michael D.
19 Burkart^{1,*}
20
21
22
23
24
25

26 ¹ Department of Chemistry and Biochemistry, University of California, San Diego, 9500 Gilman
27 Drive, La Jolla CA 92093–0358, United States
28

29 ² DOE Joint Genome Institute, Lawrence Berkeley National Laboratory, Mail Stop: 91R183, 1
30 Cyclotron Road, Berkeley, CA 94720, USA.
31

32 ³ Bigelow Laboratory for Ocean Sciences, East Boothbay ME 04544, United States
33
34

35 ⁴ University of North Alabama, Florence AL 35632, United States
36
37
38
39
40
41
42

43 * Corresponding authors: mburkart@ucsd.edu (M.D.B) and rstepanauskas@bigelow.org (R.S.)
44

45 † These authors contributed equally to the work.
46
47
48
49
50
51
52
53
54
55
56
57
58
59
60

1
2
3 **Abstract.** While thousands of environmental metagenomes have been mined for the presence of
4 novel biosynthetic gene clusters, such computational predictions do not provide evidence of their
5
6 *in vivo* biosynthetic functionality. Using a fluorescent *in situ* enzyme assay targeting carrier
7
8 proteins common to polyketide (PKS) and non-ribosomal peptide synthetases (NRPS), we
9
10 applied fluorescence-activated cell sorting to tunicate microbiome to enrich for microbes with
11
12 active secondary metabolic capabilities. Single-cell genomics uncovered the genetic basis for a
13
14 wide biosynthetic diversity in the enzyme-active cells and revealed a member of marine
15
16 *Oceanospirillales* harboring a novel NRPS gene cluster with high similarity to phylogenetically
17
18 distant marine and terrestrial bacteria. Interestingly, this synthase belongs to a larger class of
19
20 siderophore biosynthetic gene clusters commonly associated with pestilence and disease. This
21
22 demonstrates activity-guided single-cell genomics as a tool to guide novel biosynthetic
23
24 discovery.
25
26
27
28
29
30
31
32

33 **Introduction**

34
35 Antecedent discoveries of secondary metabolites have been characteristically limited to
36
37 their direct extraction from animals, plants, fungi and cultured microbes.¹ Nowadays, thousands
38
39 of genomes of uncultured microbes from a variety of environmental samples are sequenced and
40
41 mined for the presence of biosynthetic gene clusters (BGC), yet challenges still remain in the
42
43 application of this approach to complex host-associated microbiomes containing yet uncultured
44
45 bacteria.² Once a BGC is identified, the genes within these clusters can be synthesized and their
46
47 biosynthetic enzymes expressed *in vitro* in culturable hosts (Figure S1 in the Supporting
48
49 Information).³ While an attractive approach to produce a secondary metabolite without culturing,
50
51
52
53
54 considerable effort is required before one can reduce these large genomic datasets into actively
55
56
57
58
59
60

expressed biosynthetic gene clusters (BGCs) with associated secondary metabolite production.⁴

1 One of the largest issues involves the discovery of a biosynthetic pathway appropriate for *in vitro*
2 expression. While metagenome–based discoveries have revolutionized the way one can access
3 microbes at the genetic level,⁵ the presence of a biosynthetic gene cluster does not necessarily
4 mean that it is functional *in vivo*.⁶ Methods that enable sample selection based on biomarkers that
5 confirm biosynthetic activity prior to genomic analyses could accelerate discoveries of bioactive
6 molecules and increase the success with the associated bioactivity assays.
7
8
9
10
11
12
13
14

15 Here we apply fluorescent *in vivo* labeling of biosynthetic proteins as a tool to guide the
16 selection of individual microorganisms expressing secondary metabolic activities of interest
17 directly in their hosts for capture by FACS and single–cell genome sequencing. We demonstrate
18 this approach on a microbiome from the tunicate *Ciona intestinalis* (Figure 1A). This activity–
19 guided approach identifies targeted pathways in rare microorganisms without *a priori* knowledge
20 of microorganism identity or cultivation.⁷ As shown in Figure 1B, this workflow provides a
21 robust complement to current genomic sequencing approaches by applying a fluorescent *in situ*
22 biochemical readout as a tool for organism selection, a process that can be directly integrated
23 into single–cell genomics workflows.⁸
24
25
26
27
28
29
30
31
32
33
34
35

36 To demonstrate this approach, we turned to carrier proteins (CPs) and their associated 4'–
37 phosphopantetheinyltransferases (PPTases),⁹ an enzyme–substrate pair that plays a key role in
38 the biosynthesis of fatty acids (FAs), polyketides (PKs) and non–ribosomal peptides (NRPs). As
39 shown in Figure 1B, this system provides a durable model, as we have previously shown that a
40 variety of synthetic pantetheine analogues (pantetheinamides) can penetrate the cell for
41 functional activity.¹⁰ Once inside the cell, the pantetheinamide hijacks coenzyme A (CoA)
42 biosynthesis for conversion to the corresponding CoA analog and ultimately becomes site–
43
44
45
46
47
48
49
50
51
52
53
54
55
56
57
58
59
60

1
2
3 selectively tethered onto the CP by the action of a PPTase (bottom, Figure 1B).⁹ Importantly, the
4 Sfp-type PPTases, which are associated with secondary metabolism of PKS and NRPS, are well
5 known to show promiscuity for CoA identity, and therefore are excellent catalysts for labeling
6 CPs *in vivo*. Here, we demonstrate how this process can be used to isolate bacterial cells engaged
7 in active secondary metabolism (i.e., PKS and NRPS pathways) selectively over that of primary
8 metabolism (fatty acid biosynthesis, FAS) by proper gating of a solvatochromic fluorescent
9 pantetheinamide probe (DMN-P, Figure 1B).

19 Our study began by the selection of a dynamic fluorescent reporter. Developed in 2008,¹¹
20 4-dimethylnaphthalene (4-DMN) is a solvatochromic tag with a fluorescence response
21 dependent upon the hydrophobicity of its local environment.¹² In our previous studies, we used a
22 4-DMN-labeled pantetheinamide (DMN-P, Figure 1B) to probe protein-protein interactions
23 between *Escherichia coli* fatty acid synthase (FAS) carrier protein (EcACP) and its multiple
24 partner enzymes.¹³ When an EcACP is labeled with DMN-P, the probe is sequestered within the
25 hydrophobic alpha helical core of EcACP,¹³ leading to a large increase in fluorescence intensity
26 relative to that unbound in solution. Based on our previous studies,¹⁰ we anticipated that DMN-P
27 would cross the cell membranes and label CPs *in vivo*. The fact that the DMN-P was not
28 fluorescent in solution but fluoresced when protein-bound suggested that this strategy could be
29 used to directly identify cells containing the enzymatic machinery necessary to load a CP with
30 DMN-P, as illustrated in Figure 1B. The use of CP-PPTase pairs was ideally suited to develop
31 this method as CP domains are found in the majority PKS and NRPS systems.

49 **Results and Discussion**

51 We began the present study by establishing conditions to sort cells selectively based on
52 the presence of an active synthase. While bacterial cells contained fatty acid synthases (FAS), we
53
54
55
56
57
58
59
60

1
2
3 postulated that FAS ACPs would be in a steady, active *holo*-state and would not label (note that
4 the labeling method with results displayed in Fig. 1 only labels *apo*-CPs), while ACP/PCPs from
5 NRPS/PKS biosynthesis would be expressed differentially over the bacterial cell cycle, therein
6 allowing selective-labeling of their *apo*-states. Here, active NRPS/PKS cells could be sorted by
7 setting a gate just above the levels of FAS ACP labeling. Using marine rod-shaped *Bacillus sp.*
8 CNJ803 as a model, we identified conditions that provided a consistent cytosolic localization as
9 evident in Figure 1C. This was then compared with a mutant deleted in Sfp, the 4'-
10 phosphopantetheinyl transferase associated with the surfactin biosynthetic pathway in *B. subtilis*.
11 Using identical conditions, we were able to establish selectivity (compare blue in Figure 1C to
12 that of the deleted mutant in Figure 1D) and develop a gate for fluorescence-activated cell
13 sorting (FACS) as shown in Figure 1E.

14
15 We then applied this protocol on a microbiome sampled from the colonial marine
16 tunicate *Ciona intestinalis*, a model organism used in developmental biology, evolutionary
17 biology, neuroscience,^{14,15} and recently suggested as a model for microbially-associated
18 secondary metabolism.¹⁶ It was also one of the first animals to have its genome sequenced.¹⁴
19 Adjacent tunicates specimens of *Ciona intestinalis* (Figure 1A) were collected from a dock in the
20 Gulf of Maine. Freshly collected tunicates were incubated in sterile-filtered seawater along with
21 control samples of the proximal water column (WC) with either RedoxSensor Green (RSG), a
22 marker of bacterial cell viability, or the enzyme labeling DMN-P. To ensure sufficient sample of
23 microbiome cells, a total of four tunicates were pooled for each probe. After homogenization of
24 the tunicates, probe-positive cells were subjected to fluorescence-activated cell sorting (FACS,
25 Figure 1E) to deposit fluorescently-labeled cells into a 384-well microplate, one per well (see
26 Supporting Information).¹⁷ Of the $\sim 12,000 \mu\text{L}^{-1}$ viable (RSG-positive) microbial cells in its

1
2
3 tunicate homogenate, only $\sim 13 \mu\text{L}^{-1}$ (0.1%) were labeled with DMN–P stained homogenate,
4 suggesting high probe specificity. The DNA of 146–148 sorted particles per treatment was
5 amplified, sequenced and *de novo* assembled individually (Table S1 in the Supporting
6 Information).¹⁷ In total, we obtained the following number of >20 kbp genome assemblies from
7 individual, sorted particles: a) 50 of tunicate microbiome CP–expressing cells (DMN–P probe
8 positives); b) 59 of tunicate microbiome respiring cells (RSG probe positives) representing the
9 negative control without the probe; and c) 95 of adjacent seawater bacterioplankton (RGS probe
10 positives).

11
12 The phylogenetic composition of the analyzed microbial cells from the adjacent water
13 column (WC) was typical of the Gulf of Maine prokaryoplankton,¹⁸ with a predominance of
14 pelagic lineages SAR11 (*Alphaproteobacteria*) and *Flavobacteriales* (*Bacteroidetes*) (Figure 2A;
15 Table S1 in the Supporting Information). The viable microorganisms in the tunicate microbiome
16 were dominated by *Rhizobiales*, *Kordiimonadales* (*Alphaproteobacteria*), *Flavobacteriales*
17 (*Bacteroidetes*) and *Campylobacteriales* (*Epsilonproteobacteria*), which have been previously
18 shown to be associated with *C. intestinalis*.¹⁹ The DMN–P probe enriched the tunicate
19 microbiome for *Alteromonadales*, *Cellvibrionales*, *Vibrionales* and *Oceanospirillales*
20 (*Gammaproteobacteria*), which were not detectable in the total active tunicate microbiome.

21
22 The specificity of the probe was further supported by the enrichment of sequences coding
23 for PKS and NRPS synthases observed in the DMN–P sorted microbes (Figure 2B). As shown in
24 Figure 2B, antiSMASH 5.0²⁰ identified 0.77 metabolite pathways per Mbp in the RSG probe–
25 positive single amplified genomes (SAGs) and 1.17 metabolite pathways per Mbp in DMN–P
26 positive SAGs, a level that was considerably higher than the 0.47 metabolite pathways per Mbp
27
28
29
30
31
32
33
34
35
36
37
38
39
40
41
42
43
44
45
46
47
48
49
50
51
52
53
54
55
56
57
58
59
60

1
2
3 that were observed in the adjacent water column (p-value 0.024). This observation confirmed
4
5 that activity-based probes, such as DMN-P, can select microbes with biosynthetic potential.
6

7
8 Next, we explored two CPs from two different SAGs to provide evidence that the
9
10 detected CP had been truly targeted by the DMN-P probe and to confirm the CP specificity. The
11
12 first CP1, and its associated PPTase, PPT1, were obtained from a putative NRPS/Type I hybrid
13
14 gene cluster (this gene cluster was observed only in this SAG) in an *Oceanospirillales*
15
16 (*Gammaproteobacteria*) genome AH-491-C20 (red, Figure 2C), which had the highest 16S
17
18 rRNA gene similarity (97%, 80% length overlap) to *Amphritea spongicola* MEBiC0546.²¹ CP1
19
20 was chosen as it provided an excellent example of a hybrid NRPS-PKS, had a proximal PPTase,
21
22 and it contained a unique domain architecture (Figure 2C) suggesting it was a novel NRPS.
23
24

25
26 Analysis of tetramer frequencies and contig binning showed that the contig containing the NRPS
27
28 genes was similar to other contigs with *Oceanospirillales* marker genes, which excludes the
29
30 possibility that the NRPS gene cluster belonged to another co-sorted microbe or contaminating
31
32 DNA (Figure S2 in the Supporting Information). A second, unrelated CP2, was obtained from a
33
34 predicted NPRS/NRPS-like/Type I PKS cluster in a *Cellvibrionales* (*Gammaproteobacteria*)
35
36 genome AH-491-D14, with *Oceanicoccus sagamiensis* NBRC107125 as the most closely
37
38 related cultured isolate in Genbank (96% 16S rRNA gene identity, 81% overlap).²² The NRPS-
39
40 PKS CP2 was chosen, as it provided an excellent comparison with CP1.
41
42
43

44
45 *Escherichia coli* codon optimized genes were synthesized for CP1 (Figure S3 in the
46
47 Supporting Information), CP2 (Figure S4 in the Supporting Information), and PPT1 (Figure S5
48
49 in the Supporting Information), inserted into pET28a vectors, and their associated proteins were
50
51 prepared by recombinant expression in *E. coli* followed by His₆-tagged purification (Figure S6A
52
53 in the Supporting Information). Applying the method in Figure 1B *in vitro*, samples of CP1 and
54
55
56
57
58
59
60

1
2
3 CP2 were screened for their ability to be fluorescently labeled. Recombinant Sfp,⁹ a member of
4 the surfactin-type PPTase known to have a broad scope in CP labeling, was able to load DMN-P
5 onto CP1 under conditions established to label the EcACP, a positive control (Figure 2D, Figure
6 S6A in the Supporting Information). Under the initial experimental conditions, CP2 was not
7 labeled, nor was CP1 or CP2 labeled with the PPT1. Concerned that unfolding the proteins under
8 SDS-PAGE would destroy the environmentally sensitive fluorescence from the DMN-P probe,
9 we repeated the labeling process (Figure 1B) with a non-solvatochromic dye labeled CoA,
10 TAMRA-CoA.²³ Here we observed labeling of CP1 with Sfp (Figure 2E, Figure S6B-D in the
11 Supporting Information). Interestingly, PPT1 was only able to label CP1, which comes from the
12 same bacterial species. Remarkably, while Sfp could label EcACP and CP1, the fact that PPT1
13 only labeled its native substrate CP1, and not CP2 or EcACP, demonstrates the unique selectivity
14 found within PPTases.⁹

15
16
17 To explore the diversity and presence of biosynthetic gene clusters related to the
18 *Oceanospirillales* bacterium AH-491-C20 NRPS across Bacteria and Archaea in publicly
19 available genomic datasets, we used IMG/M database²⁴ (March 2020, containing 77,808
20 genomes from isolates, SAGs and metagenome assembled genomes from diverse environments)
21 and 12,715 SAGs from the GORG-Tropics data set from marine prokaryoplankton.²⁵
22 Surprisingly, the AH-491-C20 NRPS gene cluster was not present in any known members of the
23 *Oceanospirillales* order (Figure 2F), with the exception of *Zymobacter palmae*, an ethanol-
24 fermenting species isolated from palm sap,²⁶ which had moderate amino acid sequence similarity
25 (40-60%) to this gene cluster, but with a different domain organization (Figure 2C). An amino
26 acid sequence similarity below 60% and different domain organization was also found in other
27 members of *Proteobacteria* and *Firmicutes* phyla (Figure 2F). The most similar domain
28
29
30
31
32
33
34
35
36
37
38
39
40
41
42
43
44
45
46
47
48
49
50
51
52
53
54
55
56
57
58
59
60

1
2
3 organizations were found in pathogenic bacteria, such as *Vibrio cholerae* and *Vibrio mimicus*²⁷
4
5 and in marine bacteria, such as *Shewanella psychrophila* and *Photobacterium profundum*²⁸
6
7 (Figure 2C) belonging to different orders in the *Proteobacteria*. This yersiniabactin– and
8
9 vibriobactin–like cluster was not found in any of the SAGs generated using the RSG probe in
10
11 this study, which indicates the cluster’s low abundance in the total active tunicate microbiome
12
13 and highlights the utility of the activity–guided single–cell genomics for bioactive molecules.
14
15
16

17 Overall, this study demonstrates how activity–based fluorescent labeling can be coupled
18
19 with single–cell genomics to enrich for organisms expressing specific biosynthetic activity. The
20
21 usage of environmentally sensitive fluorescent probes designed to label CPs *in situ* enabled the
22
23 identification of previously undiscovered CP substrate and compatible PPTase enzyme partners
24
25 in the same, uncultured microbial cell. The use of this solvatochromic DMN–P probe provided
26
27 an enhanced response (increased fluorescence when attached to a CP⁹) that enabled selective
28
29 detection of bacteria presenting CP–containing synthases. Using model bacteria, we were able to
30
31 show that the DMN–P probe selectively labeled microbial cells and we were able to use this
32
33 signal to gate cell sorting for cells that would most likely contain an active NRPS or PKS CP–
34
35 PPTase pair. While one cannot rule out that FAS pathways may have also been labeled, our data
36
37 suggest that the application of sort gates with strict fluorescence intensity thresholds selects for
38
39 microbial cells that contain added CP–PPTase activity associated with NRPS/PKS biosynthesis.
40
41 We illustrated the enrichment for bacteria with biosynthetic activity with an example of a novel
42
43 NRPS gene cluster found in an *Oceanospirillales* species from tunicate microbiome, which was
44
45 below detection in the non–labeled control and also absent in large public repositories of
46
47 microbial genomes. While well recognized in their human health context (see homology to
48
49 *Yersinia pestis* and *Vibrio cholerae* in Figure 2C), the discovered yersiniabactin and vibriobactin
50
51
52
53
54
55
56
57
58
59
60

1 biosynthesis pathways have not been documented in *Oceanospirillales* nor tunicate microbiome
2 previously. This indicates that such novel biochemistry would remain undiscovered without the
3 use of our activity-guided single-cell genomics approach.
4

5 **Methods**

6 **Probes and materials.** Unless described otherwise, supplies and materials were obtained from
7 VWR or Fischer Scientific and used as is. The DMN-P¹³ and TAMRA-CoA²³ were prepared by
8 chemical synthesis. *E. coli* FAS ACP (EcACP) was prepared using established methods.¹³
9

10 **Microbial labeling studies.** A single colony of *Bacillus sp.* CNJ803 (a marine wild type strain)
11 or *Bacillus subtilis* 168 (a mutant deficient in Spf) was suspended in 200 μ L of A1 media. Cells
12 were then treated at 23 °C for 3 h with 500 nM DMN-P (Figure 1B) from a 100 μ M stock
13 solution of DMN-P dissolved in DMSO. Following incubation with DMN-P, nuclear stain,
14 SYTO-9 (Thermo Fisher Scientific), was added to the cultures for 15 min at a final
15 concentration of 1 μ M. Cells were spun down at 2,000 rpm for 1 min and the supernatant was
16 removed. Cell pellets were mixed with 200 μ L of 3:1 EtOH/AcOH (fixing solution) and
17 incubated for 10 min. Cells were centrifuged at 2,000 rpm for 1 min again and the supernatant
18 was removed. The cells were re-hydrolyzed with 100 μ L of water. A 20 μ L aliquot of each final
19 sample was loaded onto glass slides for super-resolution microscopy.
20
21
22
23
24
25
26
27
28
29
30
31
32
33
34
35
36
37
38

39 **Super-resolution microscopy.** Imaging was conducted on a Zeiss LSM 880 microscope with
40 FAST Airyscan using a Plan-Apochromat 63x/1.4 Oil DIC M27 objective. Blue fluorescence
41 from the DMN-P was obtained using a 405 nm laser with beamsplitters (MBS 488/561/633,
42 MBS_InVis MBS -405, DBS1 mirror, FW1 rear) and an additional 410–477 nm filter. Green
43 fluorescence from the SYTO-9 control was obtained using a 488 nm laser with beamsplitters
44 (MBS 488/561/633, MBS_InVis MBS-405, DBS1 mirror, FW1 rear). Pinhole sizes were kept
45
46
47
48
49
50
51
52
53
54

1 between 40–90 μm . Images were collected in Zen (Zeiss) with recommended gains of 700–1100,
2 digital gain of 1, depth of focus between 0.65–0.71 μm , and pixel time of 2–5 μs and image sizes
3 at 2048 \times 2048 pixels. Images were processed offline and rendered from Zen Blue (Zeiss).

4
5
6 Copies of original CZI files can be provided upon request.
7

8
9 **Specimen collection.** Live *Ciona intestinalis* were collected from 20.4 °C seawater at a depth of
10 ~0.5 m on the side of a floating dock in Boothbay Harbor Maine (Latitude 48.8, Longitude -69.6)
11 between 8:00–9:00 AM on August 29, 2018. To ensure sufficient sample size, a total of four
12 tunicates (these tunicates were collected from the same location at the same time and were
13 neighboring and attached to the same substrate) were pooled for each experiment. Immediately
14 after collection, the specimens were placed in 50 mL centrifuge tubes containing ambient
15 seawater. Additionally, ambient seawater samples were collected adjacent to tunicates in 50 mL
16 centrifuge tubes. The samples were transported to Bigelow Laboratory for Ocean Sciences at *in*
17 *situ* temperature in the dark.
18
19

20
21
22
23
24
25
26
27
28
29
30 **Activity-guided single-cell genomics.** To target cells with CP activity, four tunicates were
31 incubated in ambient seawater amended with 10 μM DMN-P at *in situ* temperature in the dark
32 for 2 h. To target all viable microbial cells, four other tunicates were incubated in 80 mL of
33 ambient seawater amended with 1 μM RedoxSensor Green (RSG, Thermo Fisher Scientific) at *in*
34 *situ* temperature in the dark for 20 min. The tunicates of each treatment were rinsed in sterile
35 Sargasso Sea water, pooled and homogenized together with 50 mL sterile Sargasso Sea water
36 using a Ninja Professional 900 W blender until the majority of the biomass was visibly
37 disintegrated. The homogenate was spun down at 2,000 rpm for 1 min and the supernatant was
38 passed through a 100 μm mesh filter. To assess the composition of the sortable microorganisms
39 in the seawater around tunicates, ambient seawater samples were labeled with a 5 μM SYTO-9
40
41
42
43
44
45
46
47
48
49
50
51
52
53
54

1
2
3 live nucleic acid stain (Thermo Fisher Scientific) for 20–40 min. Immediately before cell sorting,
4 samples were diluted 10× in sterile Sargasso Sea water. Sort gates for DMN–P probe–positive
5 cells were defined along blue fluorescence and forward scatter axes and adjusted for background
6 noise using negative (*Bacillus subtilis* 168, a mutant deficient in Sfp) and positive (*Bacillus*
7 *subtilis* 3610 DSM10, wild type) controls (culture conditions were the same as described in the
8 above section entitled Microbial isolate labeling studies). Probe–positive cells were sorted into
9 384–well plates, lysed, their DNA amplified with WGA–X, and genomes sequenced and
10 quality–controlled.¹⁷ Genome assemblies originating from multiple co–sorted cells were
11 identified and parsed using a combination of nucleotide tetramer principal component analysis
12 and homology searches in the NCBI nr database.²⁹ Biosynthetic pathways were identified with
13 antiSMASH²⁰ using KnownClusterBlast, ActiveSiteFinder and SubClusterBlast options. If
14 antiSMASH predicted multiple metabolite pathways in the same coding region, then all possible
15 products were reported.

16
17
18
19
20
21
22
23
24
25
26
27
28
29
30
31
32
33
34 **Heterologous expression of select genes/domains.** Selected domains and di–domains were
35 chosen based upon evaluation of sequencing data with antiSMASH (versions 4.2 and 5.0 were
36 used).²⁰ In particular, we selected a PPTase (PPT1) and two CP (CP1 and CP2) containing
37 sequences for recombinant evaluation. The predicted protein sequences of the full selected genes
38 were further evaluated with BLAST alignment to identify homologues and better understand
39 domain organization. In the case of CPs, disconnection locations for excised domains were
40 determined by online domain organization tools^{30,31} and by comparison with recent crystal
41 structures.^{32,33} The genes for the resulting proteins were synthesized (Twist Bioscience) and
42 cloned into a pET28a vector. With the exception of the PPTase, all genes were cloned with a 3′–
43 stop codon to provide an N–terminal His₆ tag for immobilized metal affinity purification. The
44
45
46
47
48
49
50
51
52
53
54
55
56
57
58
59
60

PPTase gene was cloned without a stop codon to provide a C-terminal His₆ tag based upon our prior experience with loss of activity with N-terminal fusions.¹¹ The identified protein sequences, gene sequences synthesized and protein sequences are provided in Figures S4–S6 in the Supporting Information.

Expression of CP1, CP2, and PPT1. The His₆-tagged proteins were expressed in *E. coli* (BL21), and grown in Terrific Broth. Cells were grown in the presence of 50 mg/L kanamycin, induced with 1 mM isopropyl β-D-1-thiogalactopyranoside (IPTG) at OD₆₀₀ = 0.8, and incubated at 16 °C for 16 h. The cell culture was spun down by centrifugation at 2,000 rpm for 30 min and the collected pellets were lysed by sonication, followed by another centrifugation at 10,000 rpm for 1 h to clear the lysate. The proteins were purified using Ni-NTA resin (ThermoFisher). Purified proteins were collected and concentrated to 2–4 mg/mL using 3 kDa (CP1 and CP2) or 10 kDa (PPT1) Amicon Ultra centrifuge filters (Millipore).

Carrier protein labeling studies. The CP labeling studies were conducted in a 30 μL reaction containing final concentration of 100 μM of the respective CP1 or CP2, 1 mM of TAMRA-CoA, and 1 μM of Sfp or PPT1 in 50 mM HEPES, 10 mM MgCl₂ pH 7.2. The mixture was gently shaken at 23 °C overnight (12 h). The resulting reactions were analyzed by 12% SDS-PAGE gel and imaged on Typhoon TRIO Variable Mode Imager (GE Healthcare BioSciences). Imaging was conducted using Cy2 (Excitation 473 nm, Emission 520 nm) for DMN-P and Cy3 (Excitation 532 nm, Emission 580 nm) for TAMRA-CoA.

References

1. Kenshole, E., Herisse, M., Michael, M. and Pidot S. J. (2021) Natural product discovery through microbial genome mining. *Curr. Opin. Chem. Biol.* 60, 47–54.

- 1
2
3 2. Palaniappan, K., Chen, I.–M. A., Chu, K., Ratner, A., Seshadri, R., Kyrpides, N. C.,
4 Ivanova, N. N., and Mouncey, N. J. (2020) MG–ABC v.5.0: an update to the IMG/Atlas
5 of biosynthetic gene clusters knowledgebase. *Nucleic Acids Res.* 48, D422–D430.
6
7
- 8 3. Wang, G., Zhao, Z., Ke, J., Engel, Y., Shi, Y.–M., Robinson, D., Bingo, K., Zhang, Z.,
9 Bowen, B., Louie, K., Wang, B., Evans, R., Miyamoto, Y., Cheng, K., Kosina, S., De
10 Raad, M., Silva, L., Luhrs, A., Lubbe, A., Hoyt, D. W., Francavilla, C., Otani, H.,
11 Deutsch, S., Washton, N. M., Rubin, E. W., Mouncey, N. J., Visel, A., Northen, T., Chen,
12 J.–F., Bode, H. B., and Yoshikuni, Y. (2019) CRAGE enables rapid activation of
13 biosynthetic gene clusters in undomesticated bacteria. *Nat. Microbiol.* 4, 2498–2510.
14
15
- 16 4. Kalkreuter, E., Pan, G., Cepeda, A. J., and Shen, B. (2020) Targeting bacterial genomes
17 for natural product discovery. *Trends Pharmacol. Sci.* 41, 13–26.
18
19
- 20 5. Miller, I. J., Chevrette, M. G., and Kwan, J. C. (2017) Interpreting microbial biosynthesis
21 in the genomic age: biological and practical consideration. *Mar. Drugs* 15, 165.
22
23
- 24 6. Li, L., Liu, X., Jiang, W., and Lu, Y. (2019) Recent advances in synthetic biology
25 approaches to optimize production of bioactive natural products in Actinobacteria. *Front.*
26 *Microbiol.* 10, 2467.
27
28
- 29 7. Martinez–Garcia, M., Brazel, D. M., Swan, B. K., Arnosti, C., Chain, P. S. G., Reitenga,
30 K. G., Xie, G., Poulton, N. J., Gomez, M. L., Masland, D. E. D., Thompson, B., Bellows,
31 W. K. B., Ziervogel, K., Lo, C.–C., Ahmed, S., Gleasner, C. D., Detter, C. J., and
32 Stepanauskas, R. (2012) Capturing single cell genomes of active polysaccharide
33 degraders: an unexpected contribution of *Verrucomicrobia*. *PLoS One* 7, e35314.
34
35
- 36 8. Doud, D. F. R., and Woyke, T. (2018) Novel approaches in function–driven single–cell
37 genomics. *FEMS Microbiol. Rev.* 41, 538–548.
38
39
40
41
42
43
44
45
46
47
48
49
50
51
52
53
54
55
56
57
58
59
60

- 1
2
3 **9.** Beld, J., Sonnenschein, E. C., Vickery, C. R., Noel, J. P., and Burkart, M. D. (2014) The
4 phosphopantetheinyl transferases: catalysis of a post-translational modification crucial
5 for life. *Nat. Prod. Rep.* *31*, 61–108.
6
7
- 8
9
10 **10.** Reyes, C. P., La Clair, J. J., and Burkart, M. D. (2010) Metabolic probes for imaging
11 endosymbiotic bacteria within toxic dinoflagellates. *Chem. Comm.* *46*, 8151–8153.
12
13
- 14 **11.** Loving, G., and Imperiali, B. (2008) A versatile amino acid analogue of the
15 solvatochromic fluorophore 4-N,N-dimethylamino-1,8-naphthalimide: a powerful tool
16 for the study of dynamic protein interactions. *J. Am. Chem. Soc.* *130*, 13630–13638.
17
18
- 19 **12.** Klymchenko, A. S. (2017) Solvatochromic and fluorogenic dyes as environment-
20 sensitive probes: Design and biological applications. *Acc. Chem. Res.* *50*, 366–375.
21
22
- 23 **13.** Charov, K., and Burkart, M. D. (2019) A single tool to monitor multiple protein-protein
24 interactions of the escherichia coli acyl carrier protein. *ACS Infect. Dis.* *5*, 1518–1523.
25
26
- 27 **14.** Satou, Y., Nakamura, R., Yu. D., Yoshida, R., Hamada, M., Fujie, M., Hisata K., Takeda,
28 H., and Satoh, N. (2019) A nearly complete genome of *Ciona intestinalis* type a (*C.*
29 *robusta*) reveals the contribution of inversion to chromosomal evolution in the genus
30 *Ciona*. *Genome Biol. Evol.* *11*, 3144–3157.
31
32
- 33 **15.** Cao, C., Lemaire, L. A., Wang, W., Yoon, P. H., Choi, Y. A., Parsons, L. R., Matese, J.
34 C., Wang, W., Levine, M., and Chen, K. (2019) Comprehensive single-cell transcriptome
35 lineages of a proto-vertebrate. *Nature* *571*, 349–354.
36
37
- 38 **16.** Leigh, B. A., Liberti, A., and Dishaw, L. J. (2016) Generation of germ-free *Ciona*
39 *intestinalis* for studies of gut-microbe interactions. *Front. Microbiol.* *7*, 2092.
40
41
- 42 **17.** Stepanauskas, R., Fergusson, E. A., Brown, J., Poulton, N. J., Tupper, B., Labonté, J. M.,
43 Becraft, E. D., Brown, J. M., Pachiadaki, M. G., Povilaitis, T., Thompson, B. P.,
44
45
46
47
48
49
50
51
52
53
54
55
56
57
58
59
60

- 1
2
3 Mascena, C. J., Bellows, W. K., and Lubys, A. (2017) Improved genome recovery and
4 integrated cell–size analyses of individual uncultured microbial cells and viral particles.
5
6 *Nat. Commun.* 8, 84.
7
8
9
- 10 **18.** Giovannoni, S. J. (2017) SAR11 Bacteria: The Most Abundant Plankton in the Oceans.
11
12 *Ann. Rev. Mar. Sci.* 9, 231–255.
13
14
- 15 **19.** Blasiak, L. C., Zinder, S. H., Buckley, D. H. and Hill, R. T. (2014) Bacterial diversity
16 associated with the tunic of the model chordate *Ciona intestinalis*. *ISME J.* 8, 309–320.
17
18
- 19 **20.** Blin, K., Shaw, S., Steinke, K., Villebro, R., Ziemert, N., Lee, S. Y., Medema, M. H. and
20
21 Weber, T. (2019) antiSMASH 5.0: updates to the secondary metabolite genome mining
22 pipeline. *Nucleic Acids Res.* 47, W81–W87.
23
24
25
- 26 **21.** Jang, H., Wang, S.–H., Seo, H.–S., Lee, J.–H., Kim, S.–J., and Kwon K. K. (2015)
27
28 *Amphritea spongicola* sp. nov., isolated from a marine sponge, and emended description
29 of the genus Amphritea. *Int. J. Syst. Evol. Microbiol.* 65, 1866–1870.
30
31
32
- 33 **22.** Park, S., Yoshizawa, S., Kogure, K., and Yokota, A. (2011) *Oceanicoccus sagamiensis*
34 gen. nov., sp. nov., a gammaproteobacterium isolated from sea water of Sagami Bay in
35 Japan. *J. Microbiol.* 49, 233–227.
36
37
38
39
- 40 **23.** Tallorin, L., Wang, J., Kim, W. E., Sahu, S., Kosa, N. M., Yang, P., Thompson, M.,
41
42 Gilson, M. K., Frazier, P. I., Burkart, M. D., and Gianneschi, N. C. (2018) Discovering de
43 novo peptide substrates for enzymes using machine learning. *Nat. Commun.* 9, 5253.
44
45
46
- 47 **24.** Chen, I. A., Chu, K., Palaniappan, K., Pillay, M., Ratner, A., Huang, J., Huntemann, M.,
48
49 Varghese, N., White, J. R., Seshadri, R., Smirnova, T., Kirton, E., Jungbluth, S. P.,
50
51 Woyke, T., Eloë–Fadrosh, E. A., Ivanova, N. N., and Kyrpides, N. K. (2019) IMG/M
52
53
54
55
56
57
58
59
60

1
2
3 v.5.0: an integrated data management and comparative analysis system for microbial
4 genomes and microbiomes. *Nucleic Acids Res.* 47, D666–D677.

- 5
6
7
8 **25.** Pachiadaki, M. G., Brown, J. M., Brown, J., Bezuidt, O., Berube, P. M., Biller, S. J.,
9 Poulton, N. J., Burkart, M. D., La Clair, J. J., Chisholm, S. W., and Stepanauskas, R.
10 (2019) Charting the complexity of the marine microbiome through single–cell genomics
11 *Cell.* 179, P1623–1635.E11.
12
13
14
15
16
17 **26.** Okamoto, T., Taguchi, H., Nakamura, K., Ikenaga, H., Kuraishi, H., and Yamasato, K.
18 (1993) *Zymobacter palmae* gen. nov., sp. nov., a new ethanol–fermenting peritrichous
19 bacterium isolated from palm sap. *Arch. Microbiol.* 160, 333–337.
20
21
22
23
24 **27.** Keating, T. A., Marshall, C. G., and Walsh, C. T. (2000) Reconstitution and
25 characterization of the *Vibrio cholerae* vibriobactin synthetase from VibB, VibE, VibF,
26 and VibH. *Biochemistry.* 39, 15522–15530.
27
28
29
30
31 **28.** Oku, N., Kawabata, K., Adachi, K., Katsuta, A., and Shizuri, Y. (2008) Unnarmicins A
32 and C, new antibacterial depsipeptides produced by marine bacterium *Photobacterium* sp.
33 MBIC06485. *J. Antibiot.* 61, 11–17.
34
35
36
37
38 **29.** Altschul, S. F., Gish, W., Miller, W., Myers, E. W., and Lipman, D. J. (1990) Basic local
39 alignment search tool. *J. Mol. Biol.* 215, 403–410.
40
41
42
43 **30.** Khater, S., Gupta, M., Agrawal, P., Sain, N., Prava, J., Gupta, P., Grover, M., Kumar, N.,
44 and Mohanty, D. (2017) SBSPKsv2: structure–based sequence analysis of polyketide
45 synthases and non–ribosomal peptide synthetases. *Nucleic Acids Res.* 45, W72–W79.
46
47
48
49 **31.** Bachmann, B. O., and Ravel J. (2009) Chapter 8. Methods for *in silico* prediction of
50 microbial polyketide and nonribosomal peptide biosynthetic pathways from DNA
51 sequence data. *Methods Enzymol.* 458, 181–217.
52
53
54
55
56
57
58
59
60

1
2
3 **32.** Miller, B. R., Sundlov, J. A., Drake, E. J., Makin, T. A., and Gulick, A. M. (2014)

4
5 Analysis of the linker region joining the adenylation and carrier protein domains of the
6
7 modular nonribosomal peptide synthetases. *Proteins* 82, 2691–2702.

8
9
10 **33.** Mitchell, C. A., Shi, C., Aldrich, C. C., and Gulick, A. M. (2012) Structure of PA1221, a
11
12 nonribosomal peptide synthetase containing adenylation and peptidyl carrier protein
13
14 domains. *Biochemistry*. 51, 3252–3563.
15
16
17
18

19 **Acknowledgments**

20
21 This study was supported by NIH R21 AI 134037 to M. D. B. and R. S. R. S. was also supported
22
23 by NSF 826734, 1441717 and 133581. M. D. and T. W. were funded by the U.S. Department of
24
25 Energy Joint Genome Institute, a DOE Office of Science User Facility, is supported under
26
27 Contract No. DE–AC02–05CH11231. We thank W. Fenical (Scripps Institution of
28
29 Oceanography, UC San Diego) for samples of *Bacillus sp.* CNJ803 used to develop the labeling
30
31 conditions and J. Piel (ETH) for the *Bacillus subtilis* strains used as positive and negative
32
33 controls. Confocal imaging was possible through the assistance of Jennifer Santini (UC San
34
35 Diego) and supported by funding from the NIH P30 NS047101.
36
37
38
39
40
41

42 **Author contributions**

43
44 K. C. prepared the samples of DMN–P; W. E. K., K. C. and J. J. L. conducted the super–
45
46 resolution imaging; E. D. B., J. B. and R. S. collected the tunicates and associated water column;
47
48 E. D. B. and J. B. prepared the microbial extracts from the tunicates; E. D. B., J. B. and R. S.
49
50 conducted the FACS analyses; E. D. B., J. B. and R. S. conducted the single–cell genomic
51
52 sequencing; E. D. B. and R. S. conducted the genome assemblies and conducted biosynthetic
53
54
55
56
57
58
59
60

1
2
3 pathway searches; E. D. B., K. C., W. E. K., M. D. B., J. J. L. and R. S. mined and selected the
4
5 CP and PPTase genes; K. C. and W. E. K. cloned and expressed the CP and PPTases; K. C. and
6
7 W. E. K. performed the CP labeling studies; M. D. and F. S. performed sequence analysis of the
8
9 NRPS gene cluster; and T. W., J. J. L, M. D. B. and R. S. organized the study. All authors
10
11 contributed to the writing.
12
13
14
15
16

17 **Supporting information**

18
19 The Supporting Information is available free of charge at:

20
21 Figures S1–S7 and experimental methods for the DMN–P FACS analyses, single–cell DNA
22
23 amplification and sequencing, SAG classification and assembly, and biosynthetic pathway
24
25 analyses have been provided. The file also contains enlarged microscopic images, gene and
26
27 protein sequences of CP1, CP2 and PPT1, and raw images of the SDS–PAGE gels. (PDF)
28
29

30
31 Table S1 (XLS)
32
33
34
35
36
37
38
39
40
41
42
43
44
45
46
47
48
49
50
51
52
53
54
55
56
57
58
59
60

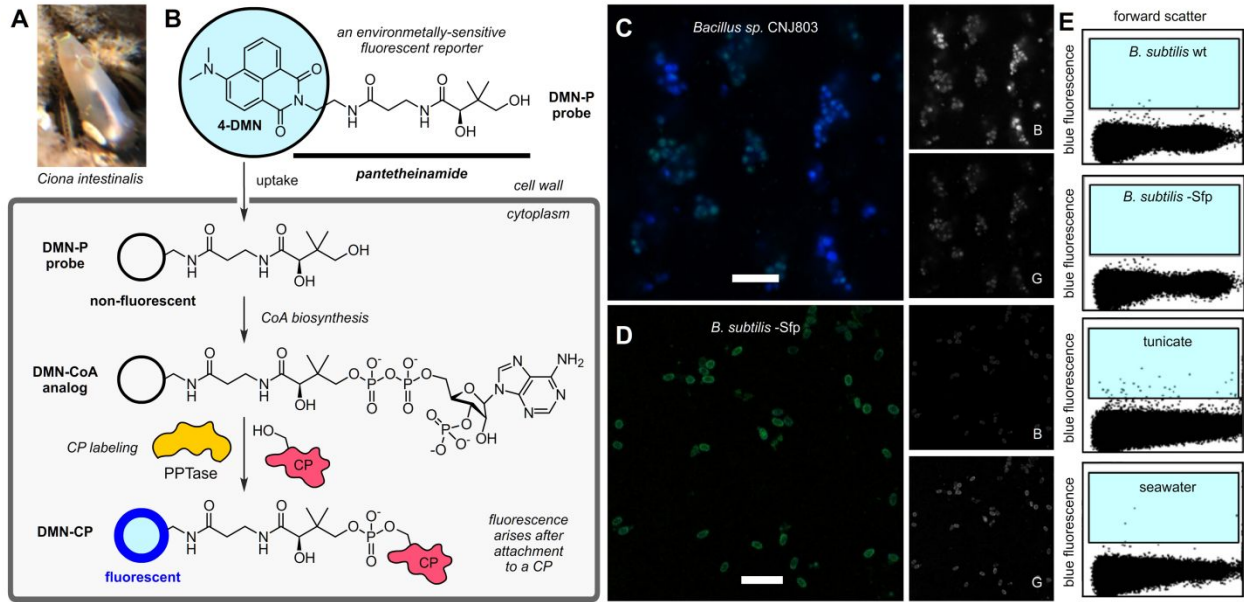


Figure 1 | Activity-guided microbial single-cell genomics. **A)** An image of the tunicate *Ciona intestinalis* specimen explored in this study. **B)** A schematic representation of the fluorescent CP labeling method used in this study. A fluorescent pantetheinamide DMN-P, designed to mimic pantetheine, is taken up by a microbial cell, where it is converted to a fluorescent-CoA analog. An environmentally sensitive fluorescent tag is used to improve the detection of protein-conjugation *in vivo*, as the 4-DMN dye used in the DMP-P probe has been shown to undergo an increase and shift in fluorescence once appended to a CP by a PPTase. **C)–D)** Super-resolution images of **C)** *Bacillus sp.* CNJ803 (a marine wild type strain) or **D)** *Bacillus subtilis* 168 (a mutant deficient in Sfp) incubated for 3 h with 500 nM DMN-P (blue) and then stained with 1 μ M nuclear SYTO-9 (green) prior to fixation and imaging. Bar denotes 5 μ m. **E)** Cells (black dots) sorted and selected (blue regions) by flow cytometry with DMN-P staining for tunicate and seawater samples. Negative (*Bacillus subtilis* 168, a mutant deficient in Sfp) and positive (*Bacillus subtilis* 3610 DSM10, wild type) controls indicate DMN-P stained cells with active CP

• PPTase pairs. (2 columns)

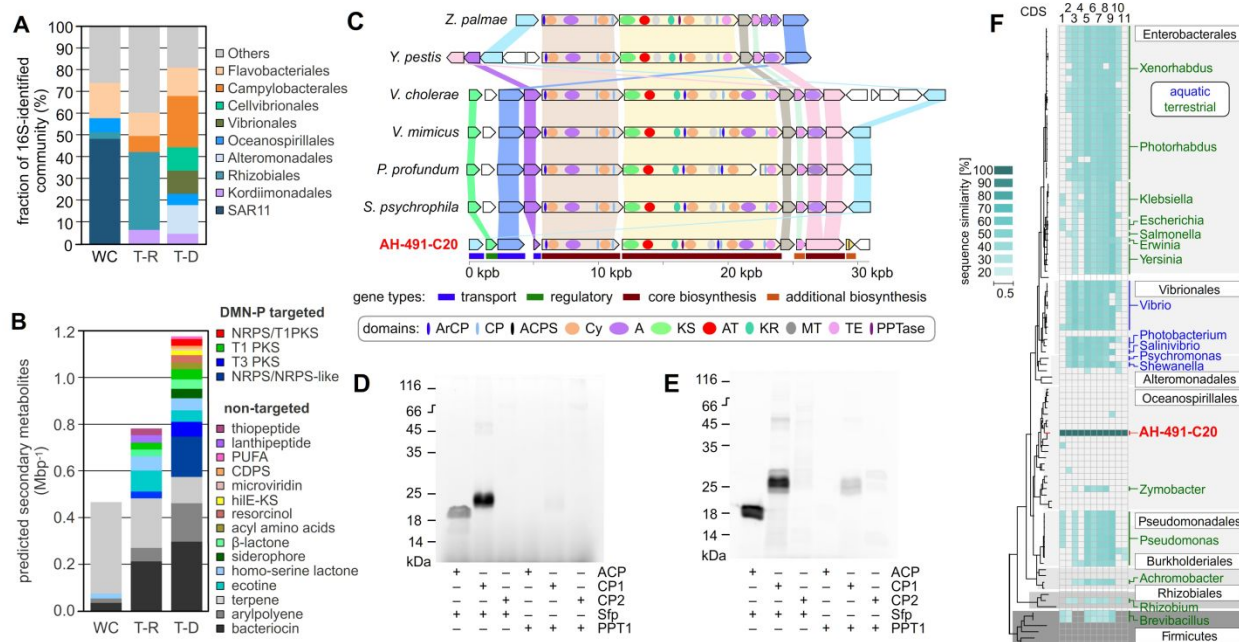


Figure 2 | Application of activity-guided single-cell genomics to mine selective CP and PPTase interactions from a tunicate microbiome. **A)** Bacterial composition and **B)** predicted secondary metabolite clusters per megabase (Mbp^{-1}) of the total microbial community in the water column (WC) compared to the viable (T-R) and DMN-P-responsive (T-D) cells in the *C. intestinalis* microbiome. *In vitro* CP-labeling analyses on the cloned and expressed CP1, CP2 and PPT1 mined from the genomic data. **C)** Visualization of the NRPS gene cluster from SAG AH-491-C20 and examples of alignments to other bacterial species which had >30% amino acid similarity on >75% of the query sequence length. **D)**–**E)** SDS-PAGE gel depicting the fluorescence in CPs after labeling by Sfp or PPT1 with **D)** DMN-P or **E)** TAMRA-CoA. *E. coli* FAS ACP (EcACP) was used as a positive control. **F)** Presence of the AH-491-C20 NRPS gene cluster across different phylogenetic groups. The phylogenetic tree includes genomes, which contained at least 7 out of 11 genes of this cluster and their closest relatives. Heatmap illustrates the level of sequence similarity for each gene. **(2 columns)**